HAL
open science

When and why sediments fail to record the geomagnetic field during polarity reversals

Jean-Pierre Valet, Laure Meynadier, Quentin Simon, Nicolas Thouveny

To cite this version:

Jean-Pierre Valet, Laure Meynadier, Quentin Simon, Nicolas Thouveny. When and why sediments fail to record the geomagnetic field during polarity reversals. Earth and Planetary Science Letters, 2016, 453, pp.96-107. 10.1016/j.epsl.2016.07.055 . hal-01419504

HAL Id: hal-01419504

https://amu.hal.science/hal-01419504v1

Submitted on 19 Dec 2016

HAL is a multi-disciplinary open access archive for the deposit and dissemination of scientific research documents, whether they are published or not. The documents may come from teaching and research institutions in France or abroad, or from public or private research centers.

L'archive ouverte pluridisciplinaire **HAL**, est destinée au dépôt et à la diffusion de documents scientifiques de niveau recherche, publiés ou non, émanant des établissements d'enseignement et de recherche français ou étrangers, des laboratoires publics ou privés.

Earth and Planetary Science Letters 453 (2016) 96–107

Contents lists available at ScienceDirect

Earth and Planetary Science Letters

www.elsevier.com/locate/epsl

When and why sediments fail to record the geomagnetic field during polarity reversals

Jean-Pierre Valet [a,*], Laure Meynadier [a], Quentin Simon [b], Nicolas Thouveny [b]

[a] Institut de Physique du Globe de Paris, Sorbonne Paris-Cité, Université Paris-Diderot, UMR 7154 CNRS, 75238 Paris Cedex 05, France
[b] CEREGE, UMR 34 Aix-Marseille Université, CNRS-IRD, 13545 Aix en Provence, France

ARTICLE INFO

Article history:
Received 8 April 2016
Received in revised form 10 June 2016
Accepted 28 July 2016
Available online xxxx
Editor: B. Buffett

Keywords:
geomagnetic reversals
magnetization acquisition
rock magnetism
sediment
demagnetization

ABSTRACT

We present four new records of the Matuyama–Brunhes (M–B) reversal from sediments of the Equatorial Indian Ocean, West Equatorial Pacific and North Atlantic Oceans with deposition rates between 2 cm/kyr and 4.5 cm/kyr. The magnetic measurements were performed using 8 cc cubic samples and provided well-defined reverse and normal polarity directions prior and after the last reversal. In three records stepwise demagnetization of the transitional samples revealed a succession of scattered directions instead of a well-defined characteristic component of magnetization. There is no relationship with changes in magnetic mineralogy, magnetic concentration and magnetic grain sizes. This behavior could be caused by weakly magnetized sediment. However the transitional samples of two cores have almost three orders of magnitude stronger magnetizations than the non-transitional samples that yielded unambiguous primary directions in the other two cores. Moreover a similar proportion of magnetic grains was aligned in all records. Therefore, the large amount of magnetic grains oriented by the weak transitional field did not contribute to improve the definition of the characteristic component. We infer that the weakness of the field might not be only responsible. Assuming that the transitional period is dominated by a multipolar field, it is likely that the rapidly moving non-dipole components generated different directions that were recorded over the 2 cm stratigraphic thickness of each sample. These components are carried by grains with similar magnetic properties yielding scattered directions during demagnetization. In contrast, the strongly magnetized sediments of the fourth core from the West Equatorial Pacific Ocean were exempt of problems during demagnetization. The declinations rotate smoothly between the two polarities while the inclinations remain close to zero. This scenario results from post-depositional realignment that integrated various amounts of pre- and post-transitional magnetic directions within each sample. The present results point out the impossibility of extracting reliable information on geomagnetic reversals from low-medium deposition rate sediments with the current sampling techniques. Among other features, they put in question the relationship between reversal duration and site latitude.

© 2016 The Authors. Published by Elsevier B.V. This is an open access article under the CC BY-NC-ND license (http://creativecommons.org/licenses/by-nc-nd/4.0/).

1. Introduction

Most paleomagnetic records of reversals has been published during the past 40 years from sedimentary sequences with accumulation rates mostly varying from 2 to 5 cm/kyr and in some very rare cases up to 10–12 cm/kyr. Despite the existence of a large database, no consensus has emerged yet concerning the structure and geometry of the transitional field, and reversal models remain controversial (Clement and Constable, 1991; Bogue and Merrill, 1992; Jacobs, 1994; Roberts, 1995; Merrill and McFadden, 1999; Constable, 2003; Amit et al., 2010; Valet and Fournier, 2016). Among various issues, a typical example was the controversy concerning the apparent tendency of virtual geomagnetic pole (VGP) paths to be confined within two preferred longitudinal bands. The longitudinal confinement of some VGP paths is puzzling when faced to the large dispersion of the transitional VGPs derived from high resolution records. This situation leads us to question the meaning of the magnetic signal recorded by sediments during reversals. This is also justified by our limited knowledge of the processes involved in sediment magnetization (see e.g. Katari and Bloxham, 2001; Tauxe et al., 2006; Shcherbakov and Sycheva, 2010; Spassov and Valet, 2012; Roberts et al., 2013). A first unknown is that magnetization depends on time required for locking-in the orientation of magnetic grains present at the same level. A second parameter is the fidelity of magnetic alignment in presence of low field intensity and a third one, barely considered, is the

* Corresponding author.
E-mail address: valet@ipgp.fr (J.-P. Valet).

http://dx.doi.org/10.1016/j.epsl.2016.07.055
0012-821X/© 2016 The Authors. Published by Elsevier B.V. This is an open access article under the CC BY-NC-ND license (http://creativecommons.org/licenses/by-nc-nd/4.0/).

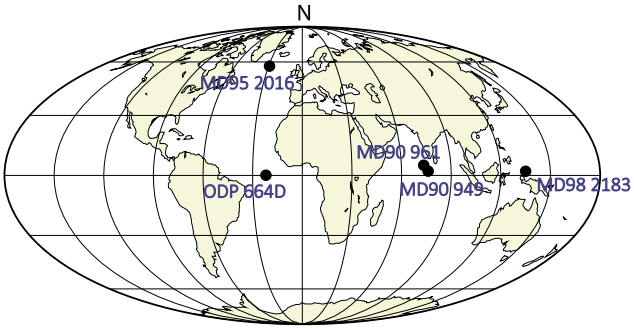

Fig. 1. Geographic locations of the four studied cores and of ODP Hole 664D.

ability of sediment magnetization at accounting for rapid field changes. It is puzzling that most transitional demagnetization diagrams are of low quality and in fact rarely discussed in detail, while they may reveal interesting information. The first question that comes to mind concerns the reproducibility of the results. Reversal records from very nearby sites (Valet et al., 1988; Van Hoof and Langereis, 1992; Van Hoof et al., 1993) have been shown to be coherent with each other, but they were recorded in similar environments, and therefore may be potentially biased by the same artifacts. The non-dipole field is reorganized substantially over a period of approximately 1 kyr (Lhuillier et al., 2011). Therefore, temporal and spatial variability of the non-dipolar field may generate different transitional field behavior at relatively distant sites. Assuming an accumulation rate of 5 cm/kyr, no more than two 8 cc cubic paleomagnetic samples describe a 1 kyr long transitional period. No critical evaluation has been proposed so far concerning the meaning of sedimentary reversal records with accumulation rates of the order of 4–5 cm/kyr because emphasis was placed on the importance of building up a large dataset. In summary, we are faced to a situation in which a large number of results has been published, while tools are missing to evaluate the fidelity of the records. In fact, we do not really know what is the potential of sediments to document polarity transitions.

A first basic approach might be to compare distinct records of the same reversal from nearby and distant locations. This would allow us to check for their consistency by combining their magnetic characteristics and their resolution. This paper analyzes four distinct records of the last reversal (Matuyama–Brunhes, M–B). Three records were obtained at equatorial sites from sediments deposited in distinct environmental conditions, and the last one comes from a high latitude North Atlantic Ocean site.

2. Core locations and samplings

Three cores were taken at the equator in the Indian and Pacific oceans. Cores MD90-949 and MD90-961 were collected during the Seymama cruise of the French R.V. Marion Dufresne in 1990 at nearby sites that differ by only 3° in latitude and longitude. Core MD90-949 (2°06.90′N 76°06.50′E) is 28 m long and was taken at 3600 m water depth. Sediment is dominated by nanofossil ooze. The site of core MD90-961 (05°03.71′N, 73°52.57′E) is located to the east of the Maldives Platform (Fig. 1). Beryllium and paleointensity measurements have documented the field intensity changes across the last reversal recorded by this sediment (Valet et al., 2014). Lithology is composed of calcareous nanofossil ooze with abundant foraminifera. The 37 m long core MD97-2183 (2°00.82′N, 135°01.26′E) was also taken by the R-V Marion-Dufresne in the western Pacific ocean and consists of hemipelagic clay with calcareous and siliceous microfossils. Previous measurements of U-channels taken from the entire core by Yamazaki and Oda (2004) helped to determine the position of the last reversal. Lastly, core MD95-2016 was obtained at high latitude (57.42°N, 370.8°E) in the North Atlantic ocean (Fig. 1) and is dominated by brown gray clay. Note that all four cores were obtained using the same coring system on board the R.V Marion-Dufresne, and therefore no large difference between records should be imputed to the coring technique. All cores were sampled using 8 cm^3 cubic plastic boxes taken adjacent to each other and in a few cases with a 1 cm overlap. No U-channel has been used to avoid additional smearing of the signal that considerably bias the transition records (Valet and Fournier, 2016).

Except in core MD95-2016, previous magnetic measurements performed on U-channels indicated the depth of the last reversal in each core (Yamazaki and Oda, 2004; Valet et al., 2014). Sediment thickness above the last reversal gives the average deposition rate at each site during the past 800 kyr. The lowest accumulation rate $v = 2.8$ cm/kyr was found at site MD90-949 and provides a resolution as low as 0.714 kyr per sample. The Indian Ocean sediment core MD90-961 has the fastest deposition rate of 4.8 cm/kyr so that each typical 2 cm thick sample integrates 0.42 kyr of geomagnetic history. Its proximity to core MD90-949 gives the opportunity of comparing two records with different resolution. Based on the B–M stratigraphic position, the average accumulation rate of the sediment from core MD97-2183 is 4.3 cm/kyr. However, the time-depth correspondence derived from the record of relative paleointensity proposed by Yamazaki and Oda (2004) suggests 3.8 cm/ka for the Brunhes chron and 7 cm/ka for the past 200 ka that, according to the authors, could reflect oversampling during coring. These two values give a field integration between 0.48 kyr and 0.52 kyr within a 2 cm sample. Lastly, core MD95-2016 from North Atlantic has an accumulation rate of 4 cm/kyr yielding a maximum resolution of 0.5 kyr per sample. Interestingly, these last three records are characterized by similar resolution. Rapid variations in deposition rates cannot be excluded, but they would be without major relevance to the conclusions and observations of the present study.

3. Demagnetization characteristics

All samples were stepwise demagnetized by alternating fields at small increments of 2 to 5 mT (depending upon evolution of their magnetic moment) until complete demagnetization between 60 and 80 mT. They were measured in four different positions using a 2G cryogenic magnetometer. In order to fully describe the evolution of demagnetization within each sequence, we show on purpose all demagnetization diagrams of the samples close to and within each transitional interval. They have been plotted in Figs. 2 and 3 using the PaleoMac software (Cogné, 2003). Further information is given in Figs. S1–S3 that show the evolution of the directions on stereoplots and the evolution of the magnetic moments after each demagnetization step. The name of each sample is given in centimeters and corresponds to its stratigraphic depth downcore. Declinations were corrected from core orientation by adjusting the mean normal declinations of the Brunhes chron to zero. Despite many demagnetization steps and care taken at isolating the characteristic component of magnetization, most demagnetization diagrams of samples close or within the transitional interval are of much poorer quality than the normal or reverse polarity samples. Below we describe the demagnetization characteristics of the samples with intermediate directions between the two polarities in each core. They are highlighted in Figs. 2 and 3.

The declination of samples between 2153 cm and 2150 cm in core MD90-949 (Figs. 2 and S1) jumps from south to north. The demagnetization diagrams show that after removing a soft overprint with positive inclination, the successive directions are highly scattered and located in two opposite quadrants of the demagnetization diagram. There is a scattered succession of directions dominated by either reverse or normal polarity. No transitional di-

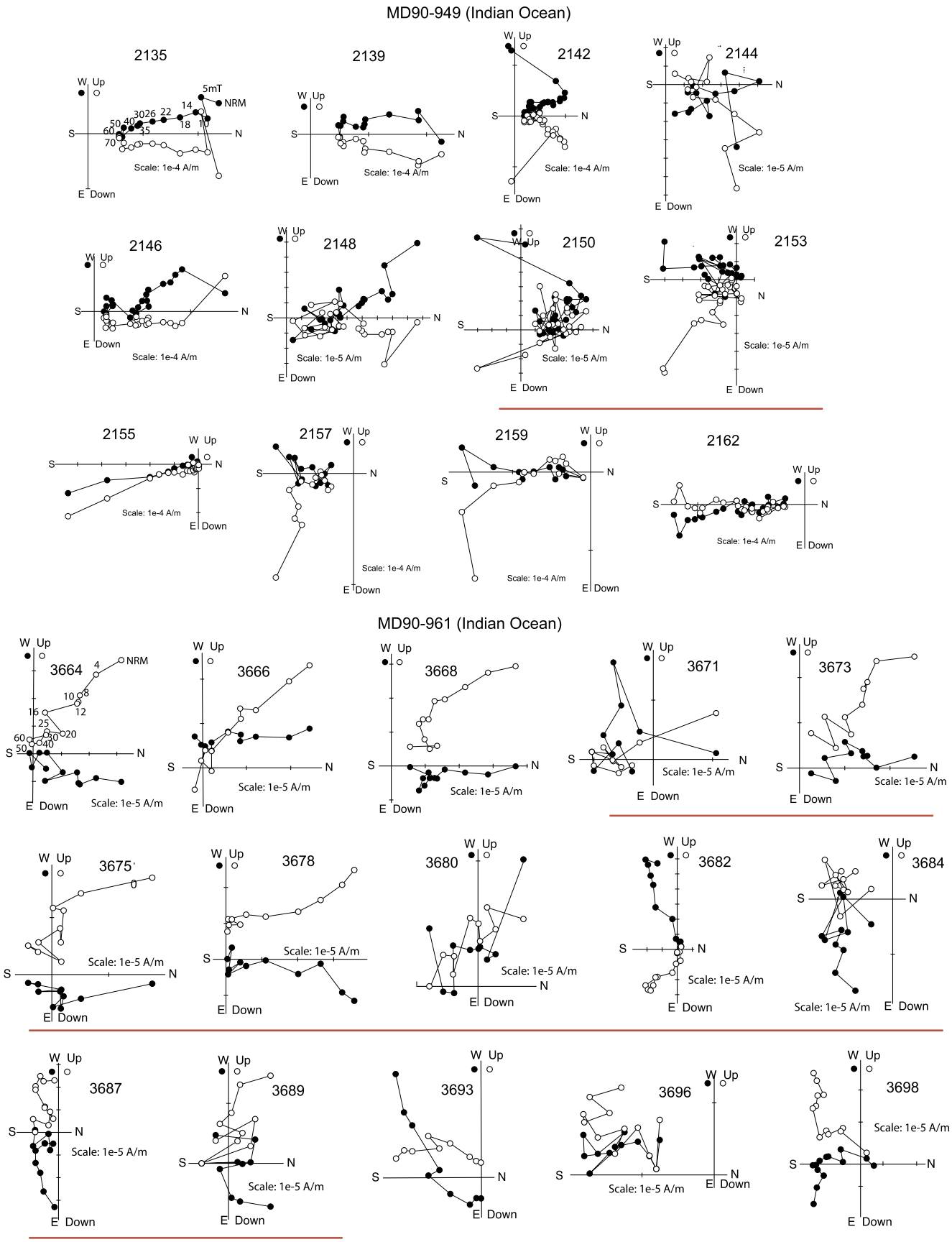

Fig. 2. Demagnetization diagrams and stereographic projections of the sample directions close and within the transitional intervals from cores MD90-949 and MD90-961. Samples corresponding to the transitional intervals are underlined. All successive directions are shown on purpose to provide a complete view of each paleomagnetic record.

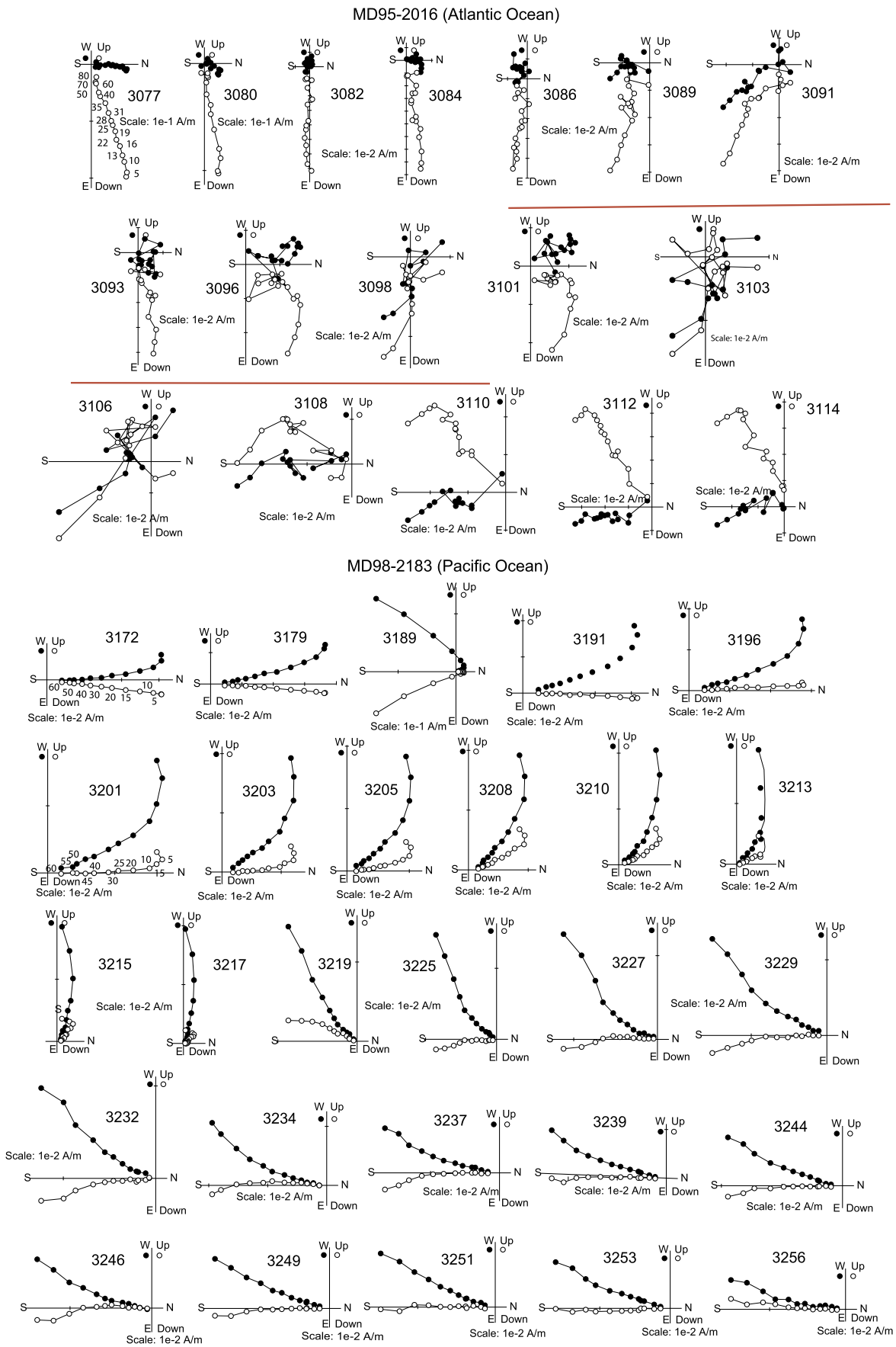

Fig. 3. Same as Fig. 2 for the samples from cores MD95-2016 and MD98-2183. The sample depths indicate the cumulative depths derived from the length of each section and do not take into account the presence of voids or elongation of the sediment.

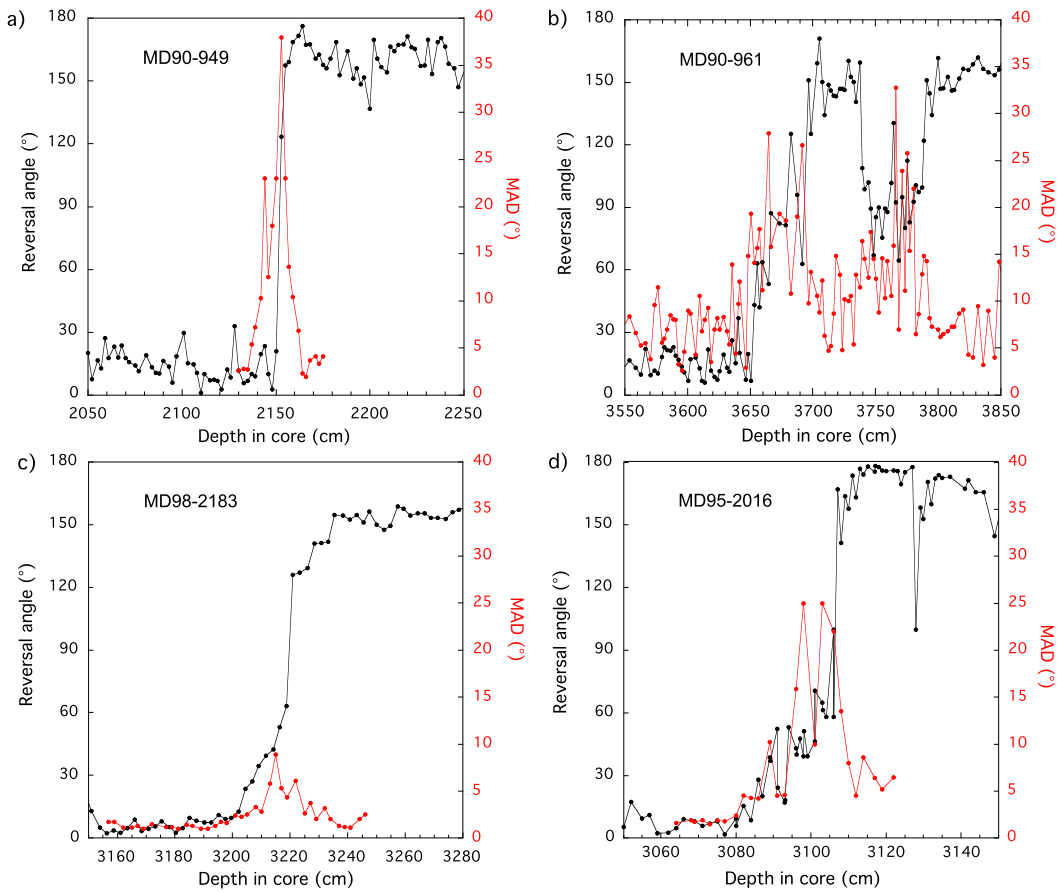

Fig. 4. Reversal angle calculated from the direction of the axial dipole at each site as a function of depth plotted along with its maximum angular deviation (MAD) as indicative of scatter of directions around the characteristic component for each transitional interval.

rection has been recorded and therefore no significant smearing has generated artificial intermediate directions. Rather the abrupt polarity change occurs over a maximum thickness of 3 cm that would suggest a very short transition.

Demagnetization performed on samples from the transitional levels of core MD90-961 (Figs. 2 and S1) frequently failed to isolate the component carrying the characteristic remanent magnetization (ChRM). Problems start above 3689 cm depth. The directions show a succession of north pointing declinations with steep inclinations and then an erratic evolution of both components. The next sample (3687 cm) exhibits a very tiny horizontal component pointing south with relatively steep inclinations after the first demagnetization steps and large scatter of declinations at the final steps. Next to it, at 3684 cm the declinations are still oriented south but demagnetization did not allow to determine an univectorial component decreasing toward the origin. Similar erratic behaviors are reproduced up to the 3668 cm level where a normal polarity characteristic direction was unambiguously indentified.

Core MD95-2016 was taken at high latitude. Before the reversal, the inclination is steep and the declination points southward (Figs. 3 and S1). Quality of demagnetization diagrams decreases gradually when approaching the transition. At 3106 cm depth, the declination is oriented south, but the inclinations are very shallow and become scattered after the third demagnetization step. The next two samples at 3103 cm and 3105 cm show successions of erratic directions during demagnetization without any clear polarity. These intervals are certainly representative of the transition, but no characteristic component (ChRM) can be isolated up to the normal polarity sample located at 3084 cm. Further insight is given by the evolution of magnetic moments (supplementary material, Figs. S1–S2) that frequently stop decreasing beyond fields as low as 15 mT within the transition zone. Resistance to a.f. demagnetization disappears progressively as we move away from the transitional interval and the magnetic moments of full polarity samples smoothly decrease during demagnetization.

The demagnetization diagrams from core MD98-2183 are in sharp contrast with the previous ones (Figs. 3 and S3). Transitional directions are nicely defined from a component that linearly decreases to the origin (or very close to it) and thus interpreted as the ChRM. The inclinations remain close to zero while the declinations rotate smoothly from south to north. At all stratigraphic levels the magnetic moments decreased regularly during demagnetization.

The low quality demagnetization diagrams within the transitional zones can be quantified by the maximum angular dispersion (MAD) for each sample. We attempted to extract a pseudo characteristic component and used each successive direction to compute the evolution of the reversal angle that represents the angular deviation from the direction of the axial geocentric dipole at the site. The reversal angles for each transition are shown as a function of depth in Fig. 4 with the MAD values derived from the demagnetization diagrams. The ChRMs that were obtained from the transitional samples are characterized by a MAD that is at least 20 times larger than outside the transitional intervals. As expected from its high quality demagnetization diagrams, the sediment from MD98-2183 is an exception to this rule.

To summarize, we identified two distinct magnetic behaviors for the samples located within the transitional intervals. The two equatorial Indian Ocean cores MD90-949 and MD90-961 and core MD95-2016 from the North Atlantic are characterized by erratic behavior of the directions during demagnetization which precludes from isolating a well-defined characteristic component. In contrast,

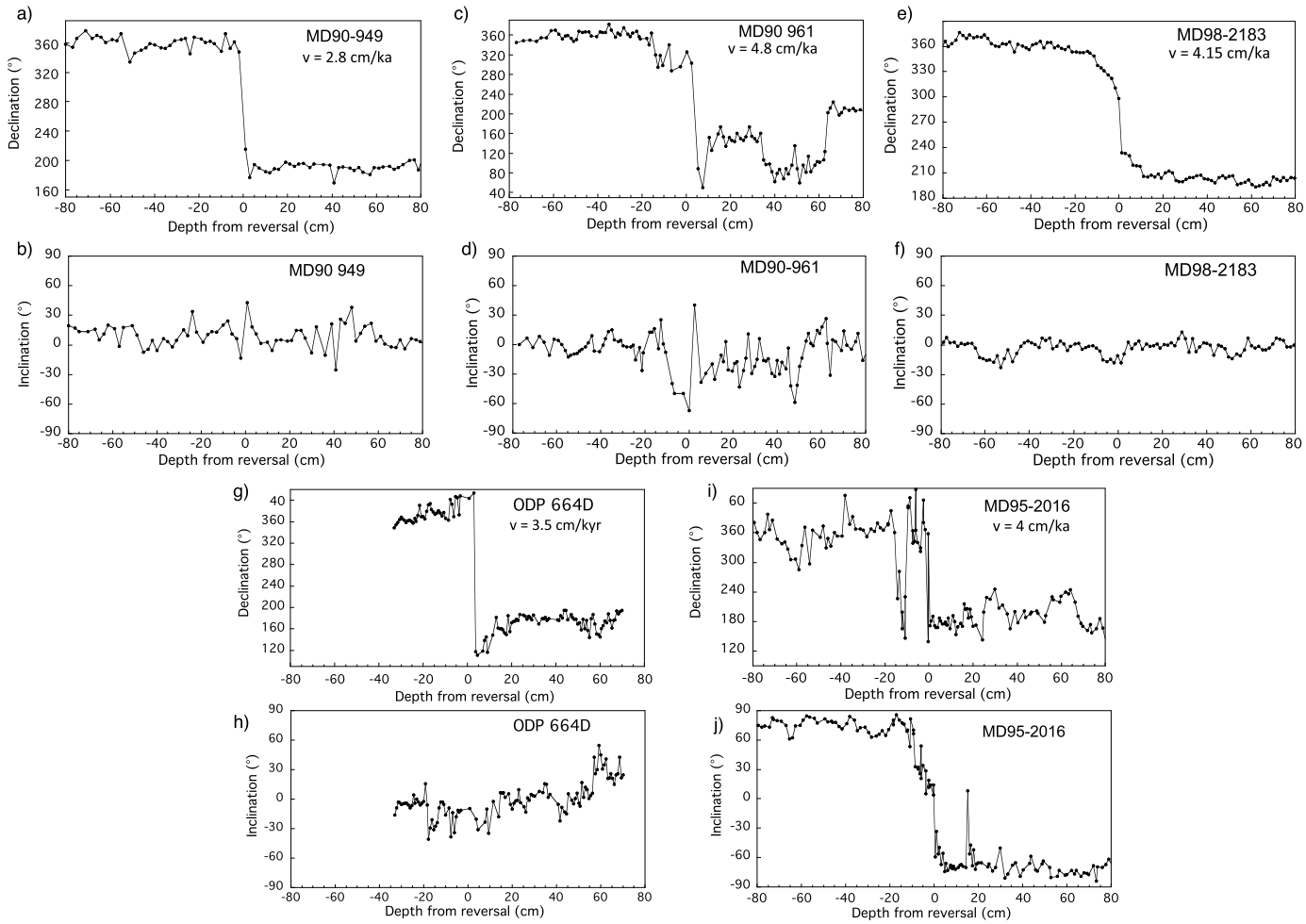

Fig. 5. Declination and inclination changes as a function of distance to mid-reversal depth that corresponds to the stratigraphic level with 90° reversal angle (see Fig. 3). Negative depths correspond to post-reversal period. The directional record from ODP Hole 664D (Valet et al., 1989) in the Eastern Equatorial Atlantic Ocean is shown for comparison.

the sediment from the West Pacific Ocean core MD98-2183 shows a nicely univectorial characteristic component that progressively rotates within the horizontal plane from south to north.

4. Directional changes and Virtual Geomagnetic Poles (VGP)

Declinations were rotated to obtain a 0° mean declination during the Brunhes period. In the absence of detailed depth–age correspondence, the records were matched on a common depth scale. The stratigraphic positions were rescaled by relying on the average deposition rate that was derived from the position of the last reversal at each site. Sediment from site MD90-949 with the lowest resolution was taken as reference. The sample depths from the other sites were thus multiplied by the ratio between their own deposition rate and the 2.8 cm/kyr value obtained for core MD90-949.

The declination and inclination variations derived from the single samples measured at each site are plotted in Fig. 5 as a function of their distance to the mid-transition point (that corresponds to the mid-reversal angle). The negative relative depth values correspond to the most recent period. The patterns of variations during each reversal differ at each site. As expected from the demagnetization diagrams, no large inclination change and no intermediate declination away from the north and south polarities define the polarity change at site MD90-949 (Fig. 5a–b). The variations displayed by the sediment from core MD90-961 (Fig. 5c–d) show a precursory episode marked by large declination changes followed by a rapid transition. The inclination is characterized by abrupt variations during both episodes. The third equatorial record from core MD98-2183 (Fig. 5e–f) shows a succession of inclination oscillations that keep the same amplitude within and outside the transition. The declination rotates regularly between the two polarities whereas there is a 60° rapid switch in the middle of the transition. For comparison, we have added the dataset of the Atlantic equatorial record from ODP Hole 664D (Fig. 5g–h) (Valet et al., 1989) that shows a rather smooth evolution of declination with an abrupt change in the middle of the transition that reminds the pattern of the record from MD98-2183 if one excludes the smoother character of this last record. The inclination displays a succession of oscillations that keep the same amplitude during the transition. Finally, the high latitude transition record from core MD95-2016 shows a progressive change from upward to downward pointing inclinations (Fig. 5i–j) with a rapid motion between negative and horizontal values. The declination reverses in two successive phases with the transition and a pronounced rebound. In both cases, few intermediate values are present between the reverse and normal polarities.

The five reversal records are characterized by different trajectories and patterns of their Virtual Geomagnetic Poles (VGPs) (Fig. 6). The VGPs from core MD90-949 (Fig. 6a) confirm the absence of transitional direction, despite a deposition rate only 1.7 times lower than at the nearby site MD90-961 (Fig. 6b). The first transitional VGPs of the precursory phase recorded at site MD90-961 are concentrated in the Southwest Pacific Ocean, and the polar-

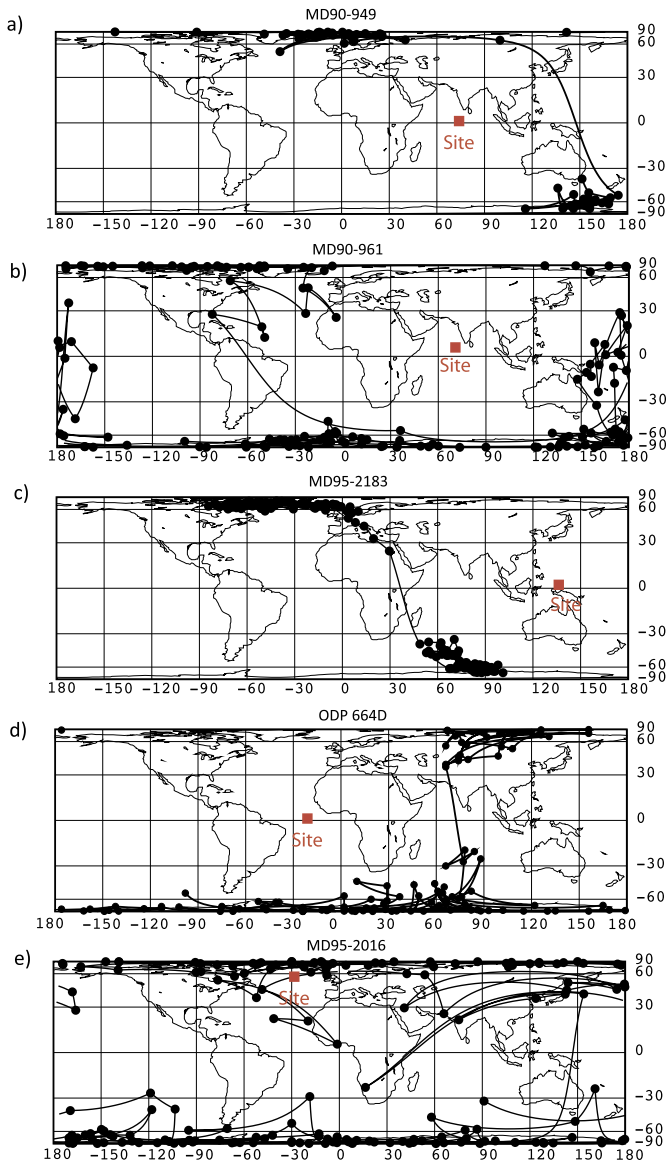

Fig. 6. VGP paths of the reversal records. The VGPs from ODP Hole 664D (Valet et al., 1989) are also shown for comparison.

ity transition is represented by VGPs that are scattered within the North Atlantic Ocean. As expected from the declination variations (Fig. 6c), the VGPs from core MD98-2183 follow a smooth and longitudinal trajectory with a cluster at the east of South East Africa, no low latitude VGPs and a succession of positions between northern Africa and northern Europe. Similarly, the record from ODP Hole 664D (Fig. 6d) does not show any VGP at low and equatorial latitudes and two mid-southern and mid-northern latitudes clusters to the west of the Indian meridian. These features are in sharp contrast with the worldwide scatter of VGPs derived from the high latitude site MD95-2016 (Fig. 6e).

5. Magnetic characteristics of transitional intervals

5.1. Coercivity and magnetic mineralogy

Several factors can influence magnetic characteristics of the records. Changes in magnetic grain sizes and/or in magnetic mineralogy could affect the sediment within the transitional intervals. Such variations could be linked to the nature of the detrital particles and therefore to environmental conditions that prevailed during this period. Climatic changes occurred on a global scale, but the core locations were associated with different paleoenvironmental conditions. It is difficult to expect similar consequences at northern and equatorial sites. Notwithstanding, this hypothesis cannot be neglected and further information can be gained from several parameters.

Table 1
Mean values of typical rock magnetic parameters across each transitional interval.

Core	S ratio		NRM/ARM	IRM/ARM
	Outside transition	Within transition		
MD90 949	0.89 ± 0.1	0.84 ± 0.05	0.17 ± 0.06	58 ± 8
MD90 961	0.97 ± 0.01	0.97 ± 0.01	0.23 ± 0.1	110 ± 15
MD98 2183	0.99 ± 0.08	0.99 ± 0.06	0.12 ± 0.06	40 ± 8
MD95 2016	0.93 ± 008	0.93 ± 0.02	0.3 ± 0.18	10 ± 6

Anhysteretic Remanent Magnetization (ARM) of most marine sediments governed by magnetite grains is on the average about ten times larger than NRM, while Isothermal Remanent Magnetization (IRM) is one order of magnitude larger than ARM. The mean IRM/ARM ratio (Table 1) is comprised between 40 and 50 for cores MD90-949 and MD98-2183, while it is around 10 for cores MD90-961 and MD95-2016. The difference could reflect the presence of larger magnetic grains within the first two cores, but both sediments behave quite differently during demagnetization. Therefore, the IRM/ARM ratio is not correlated with the magnetic behavior of the transitional samples, which makes sense since each transition was recorded by sediments of different origins.

Similarly, it is difficult to consider that changes in magnetic mineralogy were responsible for poor demagnetization of sediment during polarity transitions. The high to low coercivity ratio as expressed by the S ratio (Bloemendal et al., 1992) is similar for transitional and non-transitional intervals (Table 1). Sediment from core MD90-949 has a ratio of 0.88 ± 0.09 that indicates larger coercivity material than at the other sites with values between 0.94 ± 0.02 (MD90-961) and 0.99 ± 0.1 (MD98-2183) without significant differences between transitional and non-transitional levels. Therefore, neither differences in magnetic grain sizes, nor in magnetic mineralogy can explain the absence of a well-defined characteristic component in the transitional samples.

5.2. Influence of secondary overprint?

We can also envisage that a resistant overprint (e.g. of chemical origin) overlaps the characteristic transitional component and prevents its determination. Resistance to a.f. demagnetization and the amplitude of the secondary magnetization component can be evaluated by considering i) the amount of magnetization lost after complete removal of the overprint ii) the af peak field required to reach this step. Both indicators are plotted in Fig. 7a–d as a function of distance to mid-transition. The percent of magnetization lost is highly variable, relatively large values within transitional intervals likely result from the weak primary magnetization. They are accompanied by larger resistance to af demagnetization of the secondary component, except for core MD98-2183 that exhibits the same unblocking field of 20–25 mT at all stratigraphic levels (Fig. 7c). Overall, no large and systematic changes in coercivity suggest that a significant portion of secondary overprint overlaps the primary component.

Indirect indications about changes in coercivity can be obtained from the evolution of ARM resistance to a.f. demagnetization. The ARM is most sensitive to single domain grains and therefore to the fraction of grains carrying the NRM. If dispersion of directions during demagnetization was linked to changes in magnetic coercivity or in the amount of magnetic grains, it should be reflected by a similar evolution during ARM demagnetization. In Fig. 7f–i we compare the downcore evolutions of the amounts of ARM and

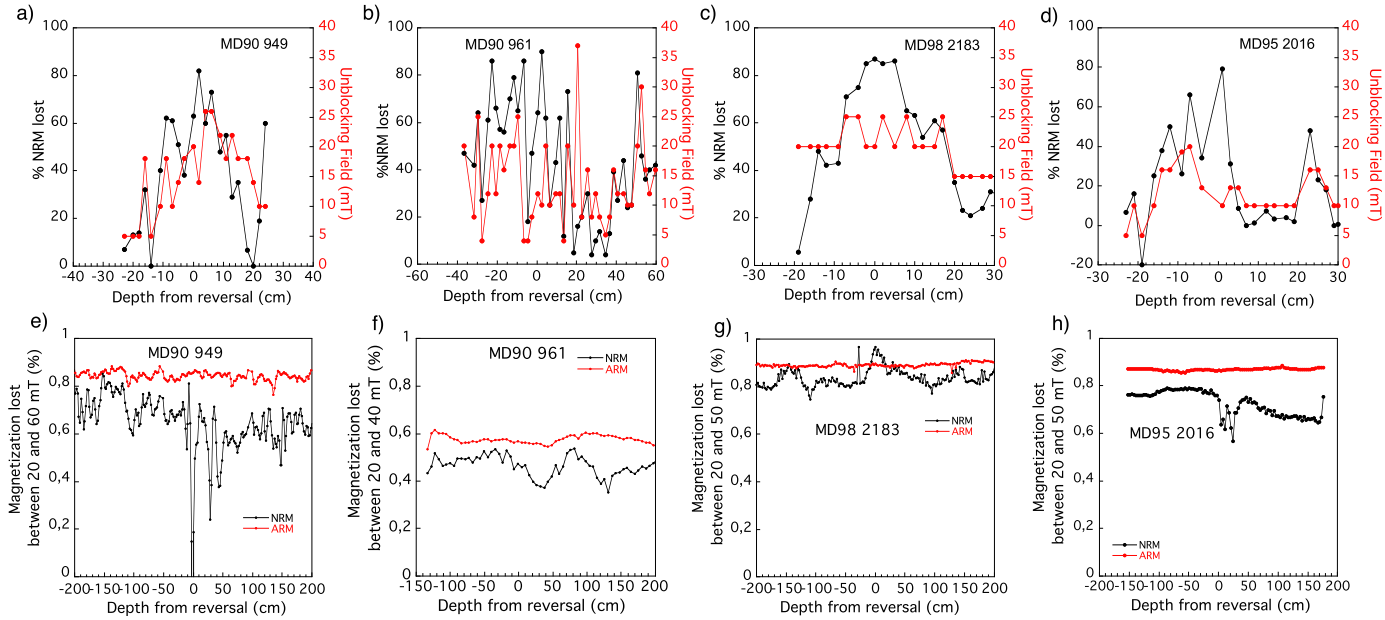

Fig. 7. Testing the potential influence of the secondary overprint: a–d) NRM lost between 0 mT and 40 or 50 mT. Evolution of the af peak field required to remove the overprint. e–h) Comparison of the amount of NRM and ARM lost between 20 mT and 40–50 or 60 mT. Resistance to demagnetization varies for NRM while it is constant for ARM. Downcore evolutions of all parameters are presented as a function of distance to mid-reversal depth.

NRM lost after demagnetization across the four transitional intervals. It is striking that the ARM shows similar resistance to af demagnetization at all levels within and outside the transitional intervals, while NRM resistance to a.f. demagnetization is weaker within transitional intervals, except again for the specific case of the MD98-2183 Pacific ocean core (Fig. 7g). Therefore, no change in rock magnetic properties can be considered as being responsible for the anomalous behavior of the transitional samples.

5.3. Magnetic concentration and magnetic moment

The weaker magnetization intensity of transitional intervals can be caused by (i) changes in magnetic mineralogy, (ii) reduction of the amount of magnetic particles, or (iii) alternatively may result from weak geomagnetic field intensity. All three factors can also act together. We already discussed the absence of significant change in magnetic mineralogy and grain sizes. Changes in magnetic concentration would be reflected by changes in ARM and SIRM, but none of these indicators revealed significant variations between the full polarity intervals and the transitional zones.

Two possibilities remain. The existence of a threshold below which the number of magnetic moments becomes too low for statistical proper alignment of the magnetic particles by the field is discarded by comparing the magnetization intensities of the cores. The transitional samples from site MD95 2016 are almost 1000 times more magnetic than the sediment from cores MD90-961 and MD90-949 (Fig. 8). The highly magnetized samples from MD95-2016 and the weakly magnetized transitional samples from the other two sites are characterized by complex demagnetization behavior. Moreover, full polarity samples from MD90-961 and MD90-949 that are three orders of magnitude weaker than the transitional interval from MD95-2016 provide unambiguous characteristic components. The sediment from MD98-2183 is an interesting exception. It is also strongly magnetized but this time the characteristic component was very well defined in all samples. The differences in magnetic concentrations between the four sites indicated by the ARM or the IRM values are similar for the NRM (Table 1). This observation further confirms the absence of link between magnetic properties and demagnetization behavior of the transitional samples.

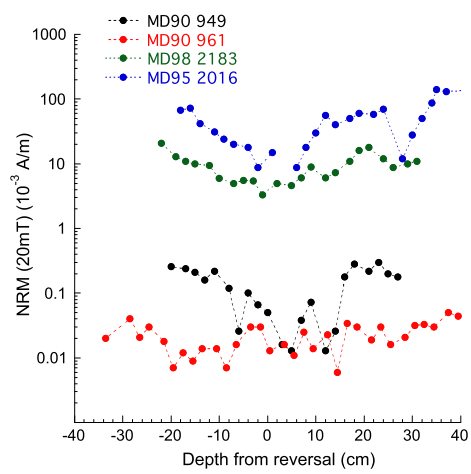

Fig. 8. Comparison of the magnetic moments within the four transitional intervals. Vertical axis is in log-scale to account for three orders of magnitude weaker magnetizations of cores MD90-949 and 961 with respect to the other two ones.

Summarizing the magnetic grains do not appear to be properly aligned by the geomagnetic field and this failure is not correlated with changes in magnetic concentration. We are thus left with the second scenario that involves the dominant contribution of the field. A different mechanism was evidently at work in the sediment from core MD98-2183. Below, we discuss which factors can generate such different situations.

5.4. Alignment of magnetic moments

Two hypotheses can be envisaged to account for the erratic demagnetization behavior of the transitional samples that has been reported in three of the four records. A first assumption is that, in presence of low field intensity the magnetic torque was not strong enough to align properly the magnetic grains along the field lines. This process is independent from magnetic concentration because the magnetic torque acting on each individual grain can only be changed by increasing or decreasing its magnetic moment and therefore by changing the size or the mineralogy of the particle.

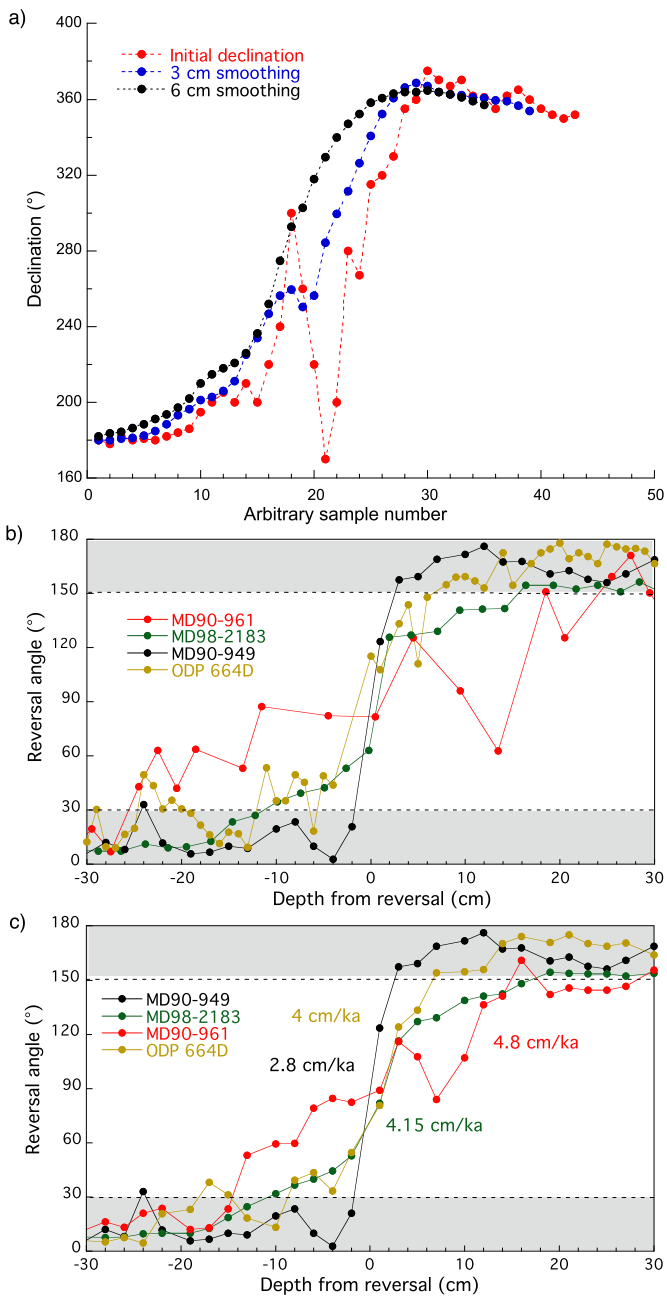

Fig. 9. a) Simulation of an equatorial reversal record by sediments with a 4 cm/ka accumulation rate and a 1.5 kyr long transition assuming smearing of the successive directions over 3 cm and 6 cm large windows (each datapoint represents 120 yrs). Reorientation of magnetic grains within a 3 cm window is enough to strongly affect the record. b, c) Reversal angle of the equatorial records (including the results from ODP Hole 664D) as a function of distance to mid-reversal depth, a) original data, b) after re-scaling the depths to those of core MD90-949 using the same deposition rate, c) after time-averaging the directions in accordance to the resolution of MD90-949.

The argument in favor of this interpretation is obtained by comparing the mean values of the NRM/ARM ratios of the records from cores MD90-949 and 961 with those from core MD95-2016. Since we are dealing with the same time intervals the field contribution to the NRM/ARM ratio was similar at the three sites. It is striking that despite three orders of magnitude difference between the moments of strongly and weakly magnetized transitional intervals, the NRM/ARM ratios have similar values (Table 1), which indicates that a similar small proportion of magnetic grains has been aligned by the field at all sites. In summary, despite similar processes acting in all cases, thousand of times more grains were oriented in core MD95-2016 than in the other two ones but this large difference did not contribute to improve the demagnetization of the samples. We infer that the demagnetization behavior is not linked to the magnetization process, nor does it depend on the magnetic characteristics of the samples, but appears to be related to the magnetic field itself. The first constraint is the presence of weak geomagnetic intensity during the transition that reduces the magnetic torque acting on each individual magnetic grain. However, one rather expect a better definition of the characteristic components in presence of strong magnetization due to the large population of oriented grains and this is not the case. Another parameter that warrants attention is field geometry. There are strong evidences from the detailed volcanic records of reversals (Jarboe et al., 2011; Valet and Fournier, 2016) that a complex rapidly changing non-dipole field becomes dominant during the short transitional period. The timescales of the non-dipole field are associated with a secular variation constant of the order of 500 yr (Lhuillier et al., 2011) which means that the field has been completely reorganized over a 1 kyr period. This is inconsistent with the timing inherent to magnetization lock-in over 2 cm of sediment. Because of these fast variations, magnetic grains with similar demagnetization spectra record different field directions within each 2 cm thick sediment slice deposited during the transition. The chaotic succession of directions during demagnetization is caused by the absence of a dominant component once the tiny soft secondary magnetization has been removed. We noted that the MAD parameter (Fig. 4) peaks in the middle of the transition when the non-dipole components are dominant. It is also significantly lower in presence of the weak dipolar field immediately before and after the transition i.e. in presence of slow field changes, pointing out the impact of fast varying directions.

This explanation cannot account for the smooth and regular evolution of the transitional directions isolated from the sediment of core MD98-2183. These characteristics combined to those of the VGP path shown in Fig. 6 could be directly interpreted in terms of rotation of the axial dipole between the two polarities. Interestingly, all intermediate directions measured at all demagnetization steps in core MD98-2183 (Fig. S3) are distributed along the western equatorial circle. The declinations rotate smoothly from south to north, while the inclinations stay close to zero. Therefore, both secondary and primary declinations follow the same path. We now have to explain why these transitional directions are so well-defined with respect to the B–M records from the Indian and Atlantic Ocean, including the equatorial records. To our knowledge, such a smooth evolution of the declinations combined to stable inclinations remaining close to zero was rarely reported in transition studies. Note that this behavior is opposite to the complex evolution of transitional directions recorded by volcanic sequences (Jarboe et al., 2011; Valet et al., 2012).

Similar behavior of transitional directions has been observed in a few attempts at simulating the consequences of long-term post-depositional reorientations of magnetic grains (Meynadier and Valet, 1996). Typical cases were reported by several authors (Coe and Liddicoat, 1994; Van Hoof and Langereis, 1992; Langereis et al., 1992) who pointed out the bias induced on transitional directions by integrating magnetic grains with reversed and normal directions in various amounts. Because reversed and normal polarity components were acquired in stronger field than the transitional components, they largely dominate the resultant magnetization. Intermediate directions are artificially generated by the coexistence of reverse and normal components that are present in various amounts within each sample.

We have simulated this process on a 1.5 kyr long equatorial transition (Fig. 9a) record that would be characterized by a rotation of the declination interrupted by a large swing and a

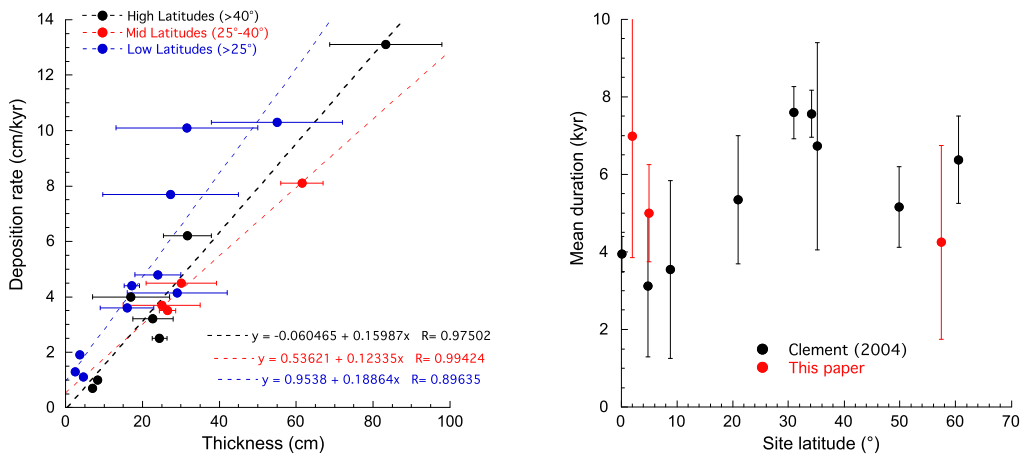

Fig. 10. a) Relationship between deposition rate and thickness of the transitional zone for all B–M records in Clement (2004) database (black dots) and the present data (red dots). The records from core MD90-949 without transitional direction and from lake Tecopa (remagnetized) were both removed. Linear fits correspond to data from low (blue), medium (red) and high latitude (black) sites, respectively. Note the influence of low deposition rate records on the slope of the fits; b) reversal duration as a function of site latitude for the same records as in (a) after removing data with accumulation rates lower than 3 cm/ka.

gradual field intensity decrease reaching ten percent of its pre-reversal value before recovering with the new polarity. In Fig. 9a we show that depths windows as small as 3 cm and 6 cm are large enough to smear out the transitional changes recorded by sediments with a 4 cm/kyr accumulation rate. This process has generated a progressive rotation of declination similarly to the data from MD95-2183. Note that the results remain globally unchanged whatever the magnetization blocking profile. The processes generating such heavy smearing remain to understand. We have seen that it is most likely not caused by peculiar magnetic grain size and/or mineralogy. The sedimentary fraction and/or the depositional conditions played certainly a major role.

6. Constraints on reversal duration

Failure to provide reliable successions of transitional directions lends doubt regarding our ability at defining the reversal boundaries, hence the apparent duration of the reversal in each record. Despite this potential limitation, we investigated whether these new records can be used to provide further constraints on reversal duration. We made the assumption that the last reverse and the first normal polarity directions may have remained geomagnetically significant. We evaluated first the durations derived from the three equatorial reversal records to which we added the data from the equatorial Atlantic Ocean ODP Hole 664D. All records are supposed to provide more or less similar durations, differences can result from the configuration of the non-dipole field at their site. As one data point represents at least 400 yr of geomagnetic history the boundaries of the transitional interval are poorly defined. In Fig. 9b are plotted the reversal angles as a function of distance to mid-reversal depth. The stratigraphic thickness of each transitional interval incorporates the directions lying more than 30° away from the direction of the axial dipole, i.e. basically outside the range of secular variation. Therefore, each transitional interval represents the thickness of sediment comprised between 30° and 150° angular deviation, and these two limits can easily be defined graphically. The data were rescaled to the same low resolution of core MD90-949, which is equivalent to dating each level using the same deposition rate. There was persisting disagreement between the apparent durations obtained after this treatment. However, reducing the resolution requires also to take into account additional smearing of directions over each sample depth. We integrated the directions within the MD90-949 equivalent sample thickness. The pattern of changes recorded at ODP site 664D is now closer to those from cores MD95-2183 and MD90-961 (Fig. 9c), but there are persisting differences that point out the large uncertainties on the lower and upper reversal limits.

After calculating the respective durations of the sedimentary records for the four more recent reversals, Clement (2004) reported that the apparent duration of transitional intervals (defined from the thickness of sediment with intermediate directions) varies with site latitude. Shorter durations are observed at low latitude sites and longer durations at equatorial and mid-latitudes. As there is no obvious reason that all reversals have the same duration, it is more reasonable to focus on a specific reversal to investigate this dependence. The last reversal is better documented than any other, and we thus took the opportunity of the present four new B–M records to test this relationship further. We used the B–M database of Clement (2004) after removing the remagnetized record from Lake Tecopa (Valet et al., 1989; Larson and Patterson, 1993) and included the present records except those from MD90-949 that has no transitional direction. The distribution of site latitudes is not uniform with a larger amount of sites lower than 20°, a grouping around 35–45° and a few cores at higher latitudes but below 60°. Deposition rates vary from less than 1 cm/kyr up to 13 cm/kyr. Given the rapidity of the reversal we consider that lower resolution than 700 yr cannot reasonably account for differences of the order of 1 or 2 kyr.

In Fig. 10a we plot the deposition rate as a function of transition thickness for all records (the three southern hemisphere sites were given equivalent positive latitudes). Reversals with similar duration should thus be distributed along a unique line. The three groups with equivalent site latitudes mentioned above are distributed along three lines with different slopes (Fig. 10a), but the lowest slope concerns the medium and not the high latitudes. As a further check on the stability of the results, we eliminated the records with deposition rates lower than 3 cm/kyr and plotted the reversal durations as a function of site latitude (Fig. 10b). Unlike Clement (2004), we found that the distribution does not increase with site latitude but rather resembles a bell pattern that peaks at 30–40° of latitude.

7. Conclusion

We investigated what confidence can be given to sedimentary records of geomagnetic reversals with deposition rates lower than 5 cm/ka that represent about 95% of the data published during the past 40 years. The approach relied on a comparison of multi-

ple records of the last reversal from one high latitude and three equatorial sites. All measurements were performed on single samples after stepwise a.f. demagnetization. After removal of a soft overprint, three of the four transitional intervals were characterized by a succession of scattered directions that impeded a proper determination of their characteristic component. We did not find evidence for significant downcore changes in magnetic mineralogy, coercivity and magnetic grain sizes between full polarity and transitional intervals. The magnetization of the transitional samples differed by up to three orders of magnitude between cores but the percentage of oriented magnetic grains was similar for highly and weakly magnetized transitional samples. Therefore, the number of oriented grains cannot be fully responsible for the poor definition of the characteristic component. It is also not straightforward to envisage the process by which a low transitional geomagnetic field would generate erratic magnetic behavior for strongly as well as for weakly magnetized samples. We favor the hypothesis that the rapidly changing non-dipole field during the reversal was inconsistent with the slow timing of magnetization lock-in. These results have direct implications for studies of geomagnetic excursions in addition to potential problems linked to post-depositional reorientations (Roberts and Winklhofer, 2004) that were nicely exemplified by the record of the fourth core MD98-2183 from the western equatorial Pacific. In this case the progressive rotation of the vector is easily simulated by the smearing of the geomagnetic signal generated by post-depositional progressive reorientations. To summarize, we identified two kinds of recordings, but both yield erroneous features of the reversing field. The first one is by far the most frequent and should hopefully be addressed by very high resolution sampling, while the second one is likely hopeless.

The present analysis was restrained to low-medium accumulation rate records. Very few reversal records have been obtained from sediments with rapid accumulation rates (10 cm/kyr and above) from deep-sea sediments (Channell and Lehman, 1997; Channell et al., 2004; Mazaud et al., 2009) and we should exclude transitions measured using U-channels (Valet and Fournier, 2016). We must add interesting data from other environments (Liddicoat, 1982; Glen et al., 1999; Sagnotti et al., 2014), particularly from lacustrine sediments but with more complex chronology. Assuming no smearing of the signal, sampling using 8 cc standard paleomagnetic cubes with a 10 cm/kyr accumulation rate yields a 200 yr resolution for a 1 kyr long transition which is similar to characteristic times of non-dipolar components (Lhuillier et al., 2011) that would be integrated over a 2 cm sample thickness. We are inclined to consider that measurements of very thin sediment layers remain the most promising future for reversal studies.

Acknowledgements

This study is supported by the ERC advanced grant GA 339899-EDIFICE under the ERC's 7th Framework Program (FP7-IDEAS-ERC). Data are available upon request at valet@ipgp.fr. This is IPGP (CNRS UMR 7154) contribution number 3777.

Appendix A. Supplementary material

Supplementary material related to this article can be found online at http://dx.doi.org/10.1016/j.epsl.2016.07.055.

References

Amit, H., Leonhardt, R., Wicht, J., 2010. Polarity reversals from paleomagnetic observations and numerical dynamos simulations. Space Sci. Rev. 155, 293–335.

Bloemendal, J., King, J.W., Hall, F.R., Doh, S.-J., 1992. Rock magnetism of Late Neogene and Pleistocene deep-sea sediments: relationship to sediment source, diagenetic processes, and sediment lithology. J. Geophys. Res. 97, 4361. http://dx.doi.org/10.1029/91JB03068.

Bogue, S.W., Merrill, R.T., 1992. The character of the field during geomagnetic reversals. Annu. Rev. Earth Planet. Sci. 20, 181–219.

Channell, J.E.T., Curtis, J.H., Flower, B.P., 2004. The Matuyama–Brunhes boundary interval (500–900 ka) in North Atlantic drift sediments. Geophys. J. Int. 158 (2), 489–505. http://dx.doi.org/10.1111/j.1365-246X.2004.02329.

Channell, J.E.T., Lehman, H., 1997. The last two geomagnetic polarity reversals recorded in high-deposition-rate sediments drifts. Nature 389, 712–715.

Clement, B.M., 2004. Dependence of the duration of geomagnetic polarity reversals on site latitude. Nature 428, 637–640.

Clement, B.M., Constable, C.G., 1991. Polarity transitions, excursions and paleosecular variation of the Earth's magnetic field. Rev. Geophys. 29, 433–442.

Coe, R.S., Liddicoat, J.C., 1994. Overprinting of natural remanence in lake sediments by a subsequent high-field intensity. Nature 367, 57–60.

Cogné, J.P., 2003. PaleoMac: a Macintosh application for treating paleomagnetic data and making plate reconstructions. Geochem. Geophys. Geosyst. 4, 1007. http://dx.doi.org/10.1029/2001GC000227.

Constable, C.G., 2003. Geomagnetic reversals – rates, timescales, preferred paths, statistical models and simulations. In: Jones, C.A., Soward, A.M., Zhang, K. (Eds.), Fluid Mechanics of Astrophysics and Geophysics. In: Earth Core and Lower Mantle Book Series, vol. 11, pp. 77–99.

Glen, J.M.G., Coe, R.S., Liddicoat, J.C., 1999. A detailed record of paleomagnetic field change from Searles Lake, California 2. The Gauss–Matuyama polarity reversal. J. Geophys. Res. 104-B6, 12883–12894.

Jacobs, J.A., 1994. Reversals of the Earth's Magnetic Field, 2nd edition. Cambridge Univ. Press.

Jarboe, N.A., Coe, R.S., Glen, J.M.G., 2011. Evidence from lava flows for complex polarity transitions: the new composite Steens Mountain reversal record. Geophys. J. Int. 186, 580–602.

Katari, K., Bloxham, J., 2001. Effects of sediment aggregate size on DRM intensity: a new theory. Earth Planet. Sci. Lett. 186 (1), 113–122.

Langereis, C.G., van Hoof, A.A.M., Rochette, P., 1992. Longitudinal confinement of geomagnetic reversal paths as a possible sedimentary artefact. Nature 358, 226–230.

Larson, E.E., Patterson, P.E., 1993. The Matuyama–Brunhes reversal at Tecopa basin, southern California, revisited again. Earth Planet. Sci. Lett. 87, 463–472.

Lhuillier, F., Fournier, A., Hulot, G., Aubert, J., 2011. The geomagnetic secular-variation timescale in observations and numerical dynamo models. Geophys. Res. Lett. 38 (9), L09306. http://dx.doi.org/10.1029/2011GL047356.

Liddicoat, J.C., 1982. Gauss–Matuyama polarity transition. Philos. Trans. R. Soc. Lond. A 306, 121–128.

Mazaud, A., Channell, J.E.T., Xuan, C., Stoner, J.S., 2009. Upper and lower polarity transitions recorded in IODP expedition 303 North Atlantic sediments: implications for transitional field geometry. Phys. Earth Planet. Inter. 172, 131–140.

Merrill, R.T., McFadden, P.L., 1999. Geomagnetic polarity transitions. Rev. Geophys. 37 (2), 201–226.

Meynadier, L., Valet, J.P., 1996. Post-depositional realignment of magnetic grains and saw-toothed variations of relative paleointensity. Earth Planet. Sci. Lett. 140, 123–132.

Roberts, A.P., 1995. Polarity transitions and excursions of the geomagnetic field. Rev. Geophys. 33, 153–160.

Roberts, A.P., Winklhofer, M., 2004. Why are geomagnetic excursions not always recorded in sediments? Constraints from post-depositional remanent magnetization lock-in modelling. Earth Planet. Sci. Lett. 227 (3), 345–359.

Roberts, A.P., Tauxe, L., Heslop, D., 2013. Magnetic paleointensity stratigraphy and high-resolution quaternary geochronology: successes and future challenges. Quat. Sci. Rev. 61, 1–16.

Sagnotti, L., Scardia, G., Giaccio, B., Liddicoat, J.C., Nomade, S., Renne, P.R., Sprain, C.J., 2014. Extremely rapid directional change during Matuyama–Brunhes geomagnetic polarity reversal. Geophys. J. Int. 199 (2), 1110–1124.

Shcherbakov, V., Sycheva, N., 2010. On the mechanism of formation of depositional remanent magnetization. Geochem. Geophys. Geosyst. 11 (2). http://dx.doi.org/10.1029/2009GC002830.

Spassov, S., Valet, J.P., 2012. Detrital magnetization from redeposition experiments of natural sediments. Earth Planet. Sci. Lett. 351, 147–157.

Tauxe, L., Steindorf, J.L., Harris, A., 2006. Depositional remanent magnetization: toward an improved theoretical and experimental foundation. Earth Planet. Sci. Lett. 244 (3–4), 515–529.

Valet, J.-P., Laj, C., Langereis, C.G., 1988. Sequential geomagnetic reversals recorded in Upper Tortonian marine clays in western Crete (Greece). J. Geophys. Res. 93 (B2), 1131–1151.

Valet, J.-P., Tauxe, L., Clement, B.M., 1989. Equatorial and mid-latitudes records of the last geomagnetic reversa from the Atlantic Ocean. Earth Planet. Sci. Lett. 94, 371–384.

Valet, J.P., Fournier, A., Courtillot, V., Herrero-Bervera, E., 2012. Dynamical similarity of geomagnetic field reversals. Nature 490, 89–94. http://dx.doi.org/10.1038/nature11491.

Valet, J.P., Bassinot, F., Bouilloux, A., Bourlès, D., Nomade, S., Guilloux, V., Lopes, F., Thouveny, N., 2014. Geomagnetic, cosmogenic and climatic changes across the last geomagnetic reversal from Equatorial Indian Ocean sediments. Earth Planet. Sci. Lett. 397, 67–79.

Valet, J.P., Fournier, A., 2016. Deciphering records of geomagnetic reversals. Rev. Geophys. 54 (2), 410–446. http://dx.doi.org/10.1002/2015RG000506.

Van Hoof, A.A.M., Langereis, C.G., 1992. The upper Kaena sedimentary record from southern Italy. J. Geophys. Res. 97 (B5), 6941–6957.

Van Hoof, A.A.M., Vanos, B.J.H., Langereis, C.G., 1993. The upper and lower Nunivak sedimentary geomagnetic transitional records from southern Sicily. Phys. Earth Planet. Inter. 77 (3–4), 297–313.

Yamazaki, T., Oda, H., 2004. Intensity-inclination correlation for long-term secular variation of the geomagnetic field and its relevance to persistent non-dipole components. In: Channell, E.T., Kent, D.V., Lowrie, W., Meert, J.G. (Eds.), Timescales of the Paleomagnetic Field.